Effect of stimulated emission on the transport characteristics of terahertz quantum-cascade lasers

R. Sharma,[a] L. Schrottke, M. Wienold, K. Biermann, R. Hey, and H. T. Grahn
Paul-Drude-Institut für Festkörperelektronik, Hausvogteiplatz 5–7, Berlin 10117, Germany

(Received 18 August 2011; accepted 29 September 2011; published online 13 October 2011)

We investigate the effect of stimulated emission on the transport characteristics of terahertz quantum-cascade lasers operating in a frequency range between 4.3 and 4.6 THz. The impact of stimulated emission is varied by changing the mirror losses via damaging one or two facets. In the case of voltage-driven measurements, a reduction in the current density near the onset of stimulated emission is observed for the facet-damaged lasers as compared to the original one. The measurements are in qualitative agreement with results of numerical simulations including the effect of stimulated emission. © *2011 American Institute of Physics*. [doi:10.1063/1.3653262]

Quantum-cascade lasers (QCLs) are unipolar semiconductor lasers that are based on intersubband transitions in a specifically engineered heterostructure.[1] These lasers offer a promising option for terahertz (THz) sources with milliwatts of average power and a definitive tunability.[2–4] In order to achieve population inversion in these structures via engineering of the scattering and tunneling rates as well as the dipole matrix elements, the subband energies and the envelope wave functions have to be designed by varying the individual layer thicknesses.

Advanced simulations of the optical and transport properties of THz QCLs include the interaction of the electrons with the photon field[5–7] so that also the slope efficiency can be calculated. Stimulated emission may lead to a significant charge redistribution within each period of the QCL. The gain enhancement by anti-reflection coatings was investigated in Ref. 8. In this work, we report on a more straightforward approach to modify the mirror losses of QCLs by damaging the front or rear facet or both. We compare the measured and the simulated transport characteristics for two cases of low (undamaged facets) and high mirror losses (damaged facets). The experiments are first carried out with the original, undamaged QCL. In a second experiment, a QCL with one damaged facet is investigated. Finally, a QCL with two damaged facets is measured. To calculate the current density, the damaged area is subtracted from the area of the original laser ridge.

The sample was grown by molecular-beam epitaxy on a semi-insulating GaAs substrate and processed into single-plasmon waveguide ridge structures. The layer sequence of the laser, starting from the injection barrier, is given by **1.7**/3.1/**1.3**/24.4/**1.5**/14.5/**2**/11.6/**3**/9.4/**3**/7.8/**2.2**/7/**2.2**/<u>16.2</u>/**3.8**/14.8 nm. The bold and underlined numbers correspond to the barriers and the Si-doped GaAs quantum well, respectively. The laser facets were mechanically damaged by using fine tip tweezers. The length of the damaged laser ridges was determined by measuring the length of the undamaged top-metal contact using an optical microscope. The experimental configuration for continuous wave (cw) and pulsed light-current-voltage measurements consists of a voltage or current source (cw or pulsed), a pyroelectric detector, and a cryostat for low temperature measurements. The laser spectra are recorded using a Fourier transform infrared spectrometer. Since the transport characteristics shown in Fig. 1(a) almost remain unaltered on damaging one or two facets, the forthcoming discussion is mainly confined to the original laser and lasers with one or two facets damaged.

A comparison of the light-current-voltage measurements of the original ($0.10 \times 1.46\,\mathrm{mm}^2$) and two-facet-damaged

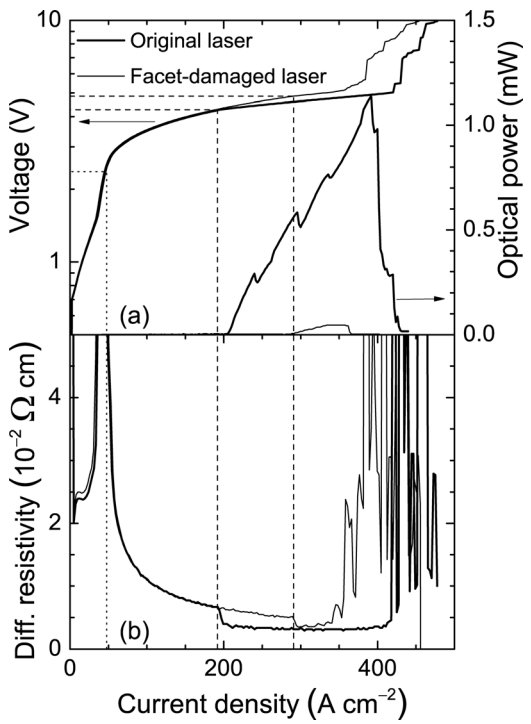

FIG. 1. (a) Continuous-wave light-current-voltage characteristics of the original (thick line) and two-facet-damaged laser (thin line) with cavity lengths of 1.46 and 1.37 mm, respectively, at 10 K. Note that the output power of the two-facet-damaged laser is about one order of magnitude smaller than for the original one. (b) Differential resistivity calculated from the data in (a) as a function of the current density of the original (thick line) and two-facet-damaged laser (thin line). The vertical and horizontal dashed lines indicate the occurrence of the first discontinuities in the differential resistivity. The vertical and horizontal dotted lines mark the onset of electron injection into the upper laser level.

[a]Electronic mail: sharma@pdi-berlin.de.

$(0.10 \times 1.37\,\mathrm{mm}^2)$ lasers is shown in Fig. 1(a) recorded at 10 K. The peak output power of the QCL is 1.1 mW. The output power of the laser is drastically reduced, when either one or two facets are damaged. The values of the threshold current densities at 10 K are 200, 279, and 294 A cm^{-2} for the original, one-facet-damaged, and two-facets-damaged lasers, respectively. Note that the transport behavior for the original and facet-damaged lasers exhibits a considerable difference above threshold (about 200 A cm^{-2}), which is a signature of the effect of stimulated emission on the transport characteristics of the investigated lasers.

In Fig. 1(b), the differential resistivity calculated from the data in Fig. 1(a) is plotted as a function of the current density. When electrons are injected into the upper laser level (above 2.5 V, cf. vertical and horizontal dotted lines in Fig. 1), the differential resistivity decreases very strongly, which is typically observed for THz QCLs (cf. Ref. 2). The first discontinuities in the differential resistivity occur at 200 and 290 A cm^{-2} (cf. vertical and horizontal dashed lines in Fig. 1) corresponding to the threshold current densities of the original and two-facet-damaged laser, respectively. Similar discontinuities in the differential resistivity have been observed for mid-infrared QCLs and related to the presence of stimulated emission.[9] Above the discontinuities, the differential resistivity remains nearly constant up to 430 and 340 A cm^{-2} for the original and the two-facet-damaged laser, respectively, where instabilities set in. The increase in the current density at a fixed voltage between the facet-damaged and original laser is partly due to stimulated emission. The actual shape of the original and facet-damaged lasers is shown by the scanning electron microscopy (SEM) images in Figs. 2(a) and 2(b), respectively.

In Figs. 3(a) and 3(b), the cw laser spectra of the original laser demonstrate that the QCL emits over a frequency range from 4.3 to 4.6 THz. A blue-shift of the central emission frequency occurs with increasing operating voltage, which is due to the Stark effect. The QCL exhibits multi-mode operation, and the number of modes depends on the operating conditions. At 210 A cm^{-2}, there are mainly three modes, while two additional modes with much weaker intensity exist on either side of the three modes. However, the number of modes increases with increasing current density [cf. Figs. 3(a) and 3(b)], which in turn results in a higher operating temperature for cw operation. In contrast, the multi-mode operation of the original laser is reduced to single-mode operation, when one facet is damaged as shown in Figs. 3(c) and 3(d). The single-mode emission can be explained by the higher threshold gain due to the increased mirror losses. With increasing current density from 340 to 390 A cm^{-2}, the emission peak of the facet-damaged QCL is shifted from about 4.52 to 4.61 THz accompanied by an increase of the operating temperature from 15 to 24 K. Note that for the facet-damaged QCL, a current density well above threshold is necessary to be able to record the emission spectra.

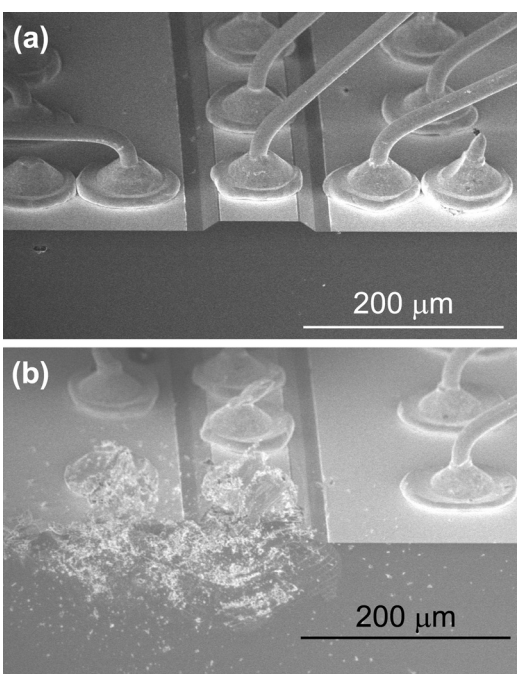

FIG. 2. SEM images of (a) the original facet and (b) the damaged facet with a ridge width of 100 μm.

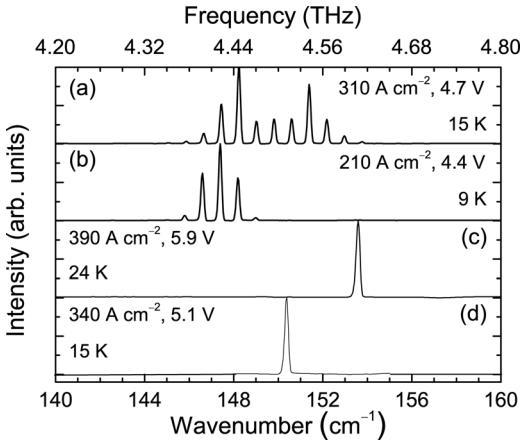

FIG. 3. Cw laser spectra of (a) and (b) the original as well as (c) and (d) the one-facet-damaged QCL.

The simulations are performed according to the model presented in Ref. 6. Hence, the effective losses $\alpha_{eff} = \alpha/\Gamma$ with $\alpha = \alpha_w + \alpha_m$ have to be determined, where Γ denotes the confinement factor, α_w the waveguide losses, and α_m the mirror losses. Assuming a reflectivity of $R_1 = R_2 = 0.3$ for each facet, we obtain a value of 8.3 cm^{-1} for the mirror losses of the original laser. The waveguide losses can be derived from the analysis of the threshold current densities for lasers with different cavity lengths L.[10] As far as the experimental part is concerned, we have measured the light-current-voltage characteristics under pulsed operation of undamaged laser stripes with cavity lengths of 1.09, 1.22, 1.46, as well as 3.47 mm and a width of 0.1 mm. The corresponding threshold current densities are 186, 172, 164, and 133 A cm^{-2}, respectively. In order to determine α_w, we plot the threshold current density as a function of $1/L$. Using the mirror losses for the original laser given above, a value of 15 cm^{-1} is determined for the waveguide losses. Since the waveguide losses are assumed to be the same in the original and facet-damaged lasers and the threshold current densities of the facet-damaged lasers are known, we can now determine the mirror losses for the one-facet-damaged and

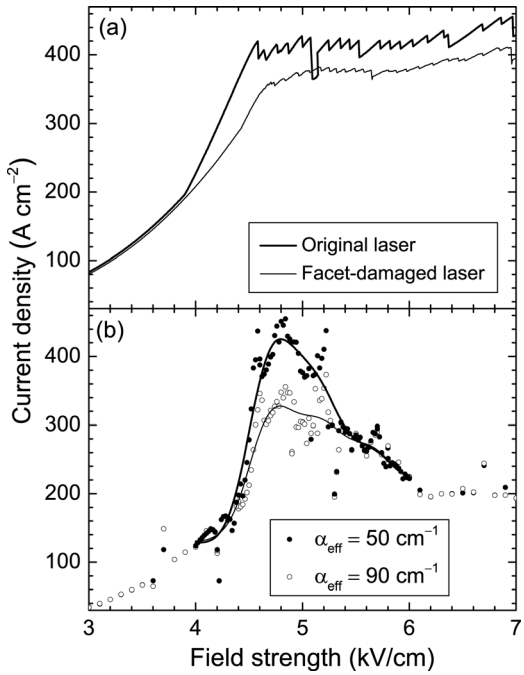

FIG. 4. (a) Measured current density as a function of average field strength for the original (thick line) and two-facet-damaged laser (thin line) at 10 K. The average field strength is calculated by dividing the applied voltage by the thickness of the active region. (b) Calculated current density for two different values of the effective losses. The solid lines are a guide to the eye.

two-facets-damaged lasers to be 21 and 26 cm^{-1}, respectively. The effective losses α_{eff} are, therefore, 52 cm^{-1} for the original laser, 80 cm^{-1} for the one-facet-damaged laser, and 91 cm^{-1} for the two-facet-damaged laser assuming $\Gamma = 0.45$.

The current density has also been measured as a function of the applied voltage at 10 K for the original and the two-facet-damaged laser. The corresponding result is shown in Fig. 4(a), where the applied voltage has been converted into an average field strength by dividing the applied voltage by the thickness of the active region. The current density of the original laser exhibits a sawtooth characteristic above 4.6 kV/cm, which is due to the onset of the formation of stationary electric-field domains (EFDs).[11] Note that only data for the up-sweep direction are shown, since no hysteresis is observed for this particular laser in contrast to previous investigations.[12] For semiconductor superlattices, the onset of EFD formation is directly related to the onset of negative differential resistance (NDR) in the drift velocity-field relation.[13] In the case of the present QCL, the onset of the domain formation occurs at a fixed voltage and is almost independent of the mirror losses. Note that EFD formation is also present in the two-facet-damaged laser, even though the current density does not display the sawtooth characteristic as clearly as for the original laser. In the simulated results shown in Fig. 4(b), the field strength of the onset of NDR does not change with stimulated emission ($\alpha_{eff} = 50\,cm^{-1}$, corresponding to the original laser) or with reduced stimulated emission ($\alpha_{eff} = 90\,cm^{-1}$, corresponding to the two-facet-damaged laser) in agreement with the experimental observation. The calculated current densities displayed in Fig. 4(b) remain unaltered for an increase of the effective losses for the field strength values of 3.0–4.6 kV/cm and 5.3–7.0 kV/cm However, a significant difference is observed in the case when stimulated emission is included in the simulations above threshold, i.e., between 4.6 and 5.3 kV/cm In this regime, an increase in the effective losses from 50 to 90 cm^{-1} results in a reduction of the current density. Since the calculation of the current densities does not include the effects of EFD formation, the results of the calculations can only be compared with the experimental results below the onset of NDR. Due to the increased mirror losses in the facet-damaged lasers, the intrinsic gain maximum of the active region has to exceed the threshold gain of 90 cm^{-1}. This result is in agreement with the numerical simulations, which predict a maximum intrinsic gain of 120 cm^{-1}.

In summary, we have experimentally probed the effect of stimulated emission on the transport characteristics of a THz QCL by increasing the mirror losses via damaging the front or rear facet or both facets of the QCL. The experimental results have been compared to the results of numerical calculations, which include the effect of stimulated emission. The reasonable agreement between the experimental and simulated threshold current densities demonstrate that the effect of stimulated emission on the transport properties of the QCL can be well reproduced by the simulations.

The authors would like to thank M. Höricke for sample growth and W. Anders for sample processing. We also acknowledge partial financial support by the European Commission through the ProFIT program of the Investitionsbank Berlin.

[1]B. S. Williams, Nature Photonics **1**, 517 (2007).
[2]S. Barbieri, J. Alton, H. E. Beere, J. Fowler, E. H. Linfield, and D. A. Ritchie, Appl. Phys. Lett. **85**, 1674 (2004).
[3]B. S. Williams, S. Kumar, Q. Hu, and J. L. Reno, Electron. Lett. **42**, 89 (2006).
[4]M. Wienold, L. Schrottke, M. Giehler, R. Hey, W. Anders, and H. T. Grahn, Appl. Phys. Lett **97**, 071113 (2010).
[5]C. Jirauschek, Appl. Phys. Lett. **96**, 011103 (2010).
[6]L. Schrottke, M. Wienold, M. Giehler, R. Hey, and H. T. Grahn, J. Appl. Phys. **108**, 103108 (2010).
[7]R. Terazzi and J. Faist, New J. Phys. **12**, 033045 (2010).
[8]R. Rungsawang, N. Jukam, J. Maysonnave, P. Cavalié, J. Madéo, D. Oustinov, S. S. Dhillon, J. Tignon, P. Gellie, C. Sirtori, S. Barbieri, H. E. Beere, and D. A. Ritchie, Appl. Phys. Lett. **98**, 101102 (2011).
[9]C. Sirtori, F. Capasso, J. Faist, A. L. Hutchinson, D. L. Sivco, and A. Y. Cho, IEEE J. Quantum Electron. **34**, 1722 (1998).
[10]C. Gmachl, F. Capasso, D. L. Sivco and A. Y. Cho, Rep. Prog. Phys. **64**, 1533 (2001).
[11]S. L. Lu, L. Schrottke, S. W. Teitsworth, R. Hey, and H. T. Grahn, Phys. Rev. B **73**, 033311 (2006).
[12]M. Wienold, L. Schrottke, M. Giehler, R. Hey, and H. T. Grahn, J. Appl. Phys. **109**, 073112 (2011).
[13]L. L. Bonilla and H. T. Grahn, Rep. Prog. Phys. **68**, 577 (2005).